Electronic Supplementary Material (ESI) for Nanoscale.

Supplementary Information

Various half-metallic nodal loops in organic $Cr_2N_6C_3$ monolayers

Hairui Bao[1], Bao Zhao[1,2], Yang Xue[3,1], Hao Huan[1], Guanyi Gao[1], Xiaojuan Liu[1], and Zhongqin Yang[1,4]*

[1]*State Key Laboratory of Surface Physics and Key Laboratory of Computational Physical Sciences (MOE) & Department of Physics, Fudan University, Shanghai 200433, China*

[2]*School of Physics Science and Information Technology, Shandong Key Laboratory of Optical Communication Science and Technology, Liaocheng University, Liaocheng 252059, China*

[3]*School of Science, East China University of Science and Technology, Shanghai 200237, China*

[4]*Collaborative Innovation Center of Advanced Microstructures, Nanjing 210093, China*

Corresponding Author

*E-mail: zyang@fudan.edu.cn

Table SI: The total energies (in eV) for FM, NM, AFM-N, AFM-ST, AFM-ZZ, and AFM-N-ST states for the $Cr_2N_6C_3$ ML without and with the Hubbard *U* (in eV) corrections.

	FM	NM	AFM-N	AFM-ST	AFM-ZZ	AFM-N-ST
U_{eff}=0	**-376.455**	-366.372	-374.942	-375.141	-375.633	-375.344
U_{eff}=3.5	**-356.944**	–	-356.348	-356.218	-356.700	-356.353

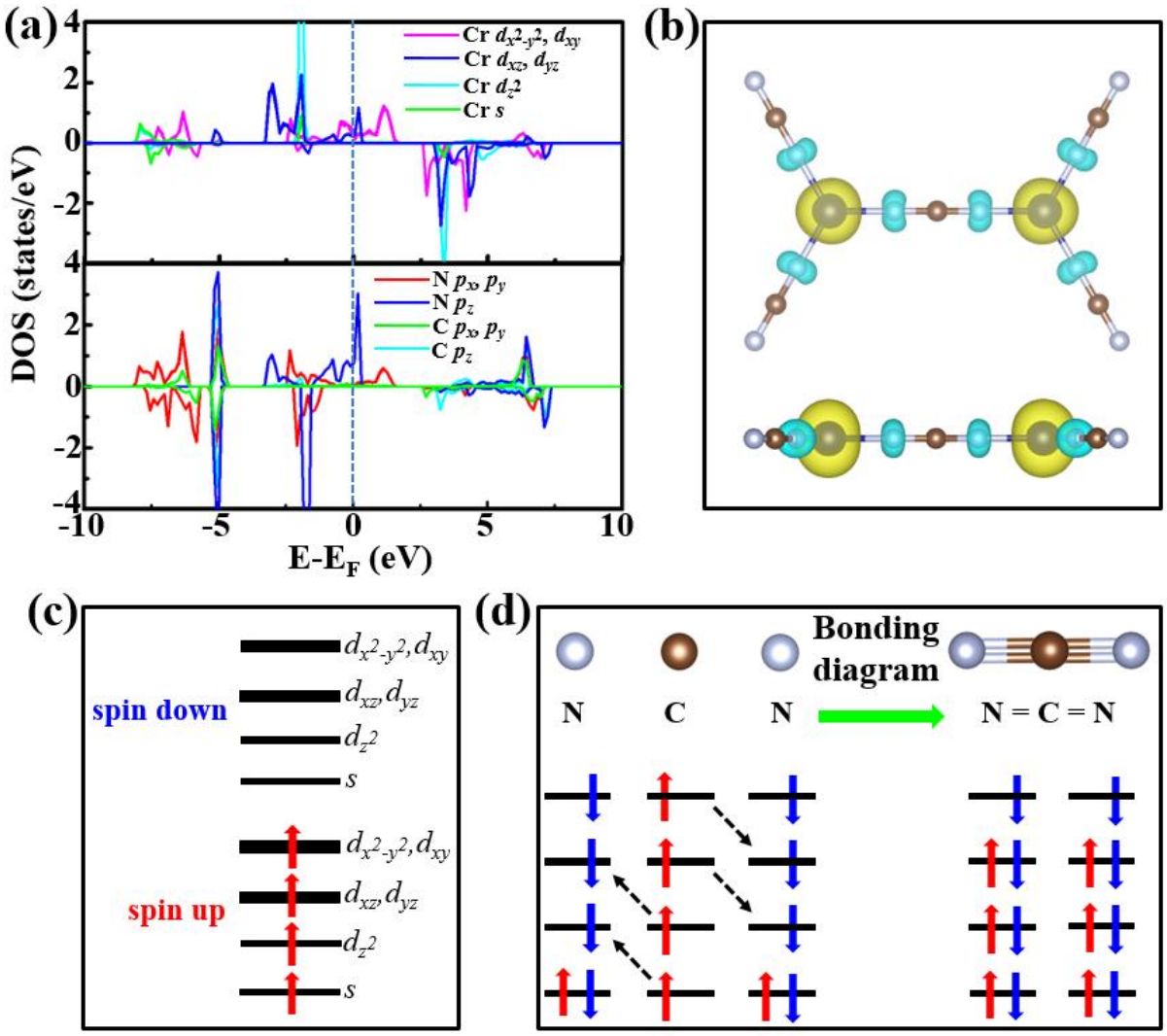

Fig. S1: (a) Orbital-resolved DOSs of the FM $Cr_2N_6C_3$ ML. The positive and negative DOS values correspond to the spin-up and spin-down states, respectively. (b) Spatial distribution of the spin-polarized electron density for the $Cr_2N_6C_3$ ML. The yellow and light blue colors denote the net spin-up and spin-down charge densities, respectively. (c) Electronic configuration of the Cr ions in the $Cr_2N_6C_3$ ML. (d) Bonding diagram of the double bonds formed between the N and C atoms.

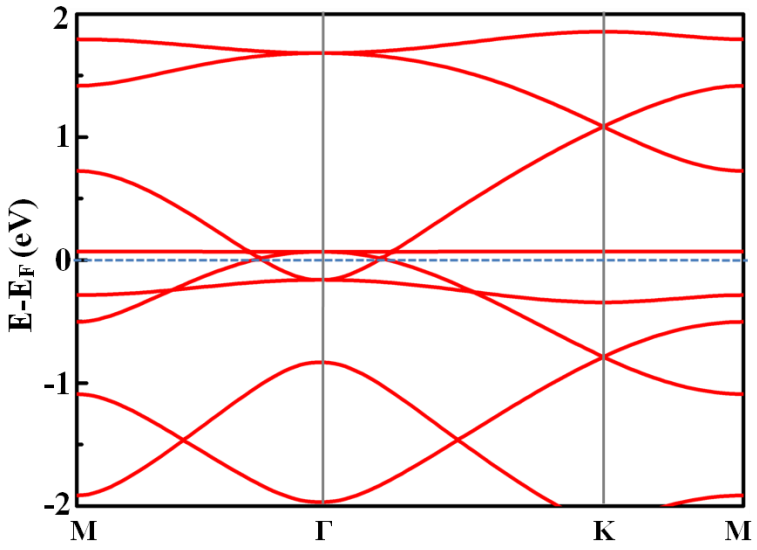

Fig. S2: Band structure of the $Cr_2N_6C_3$ ML with the HSE06 method. The SOC interaction is not considered.

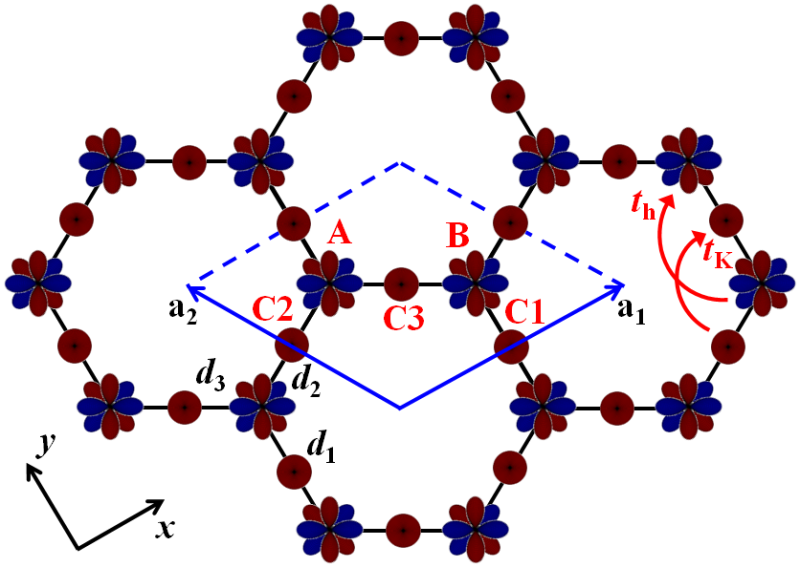

Fig. S3: The 2D honeycomb-Kagome lattice with five lattice sites per unit cell. The sites A and B both have two orbitals $d_{x^2-y^2}$ and d_{xy}, while the sites C1, C2, and C3 all have single orbitals p_z. The blue arrows denote the lattice vectors, while the red arrows represent the nearest-neighbor hoppings t_{h} and t_{K} for honeycomb and Kagome sublattices, respectively. The position vectors $\boldsymbol{d_i}$ (i=1, 2, 3) between the nearest-neighbor sites in the honeycomb sublattice are marked.

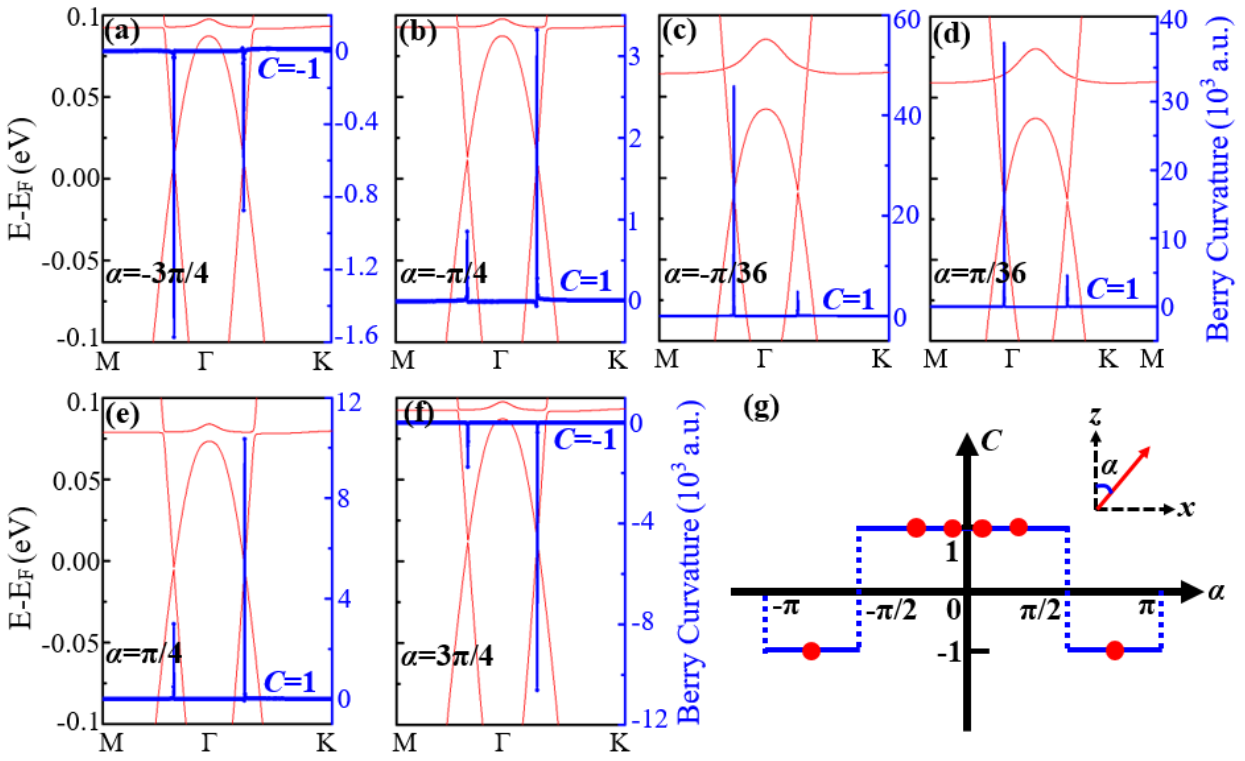

Fig. S4: (a)-(f) Band structures and Berry curvatures of the $Cr_2N_6C_3$ MLs with the magnetization direction α=-3π/4, -π/4, -π/36, π/36, π/4, and 3π/4, respectively. For the cases of α=-π/36 and π/36, the SOC strength is tripled to obtain clear results. (g) The Chern number as a function of the magnetization direction α.

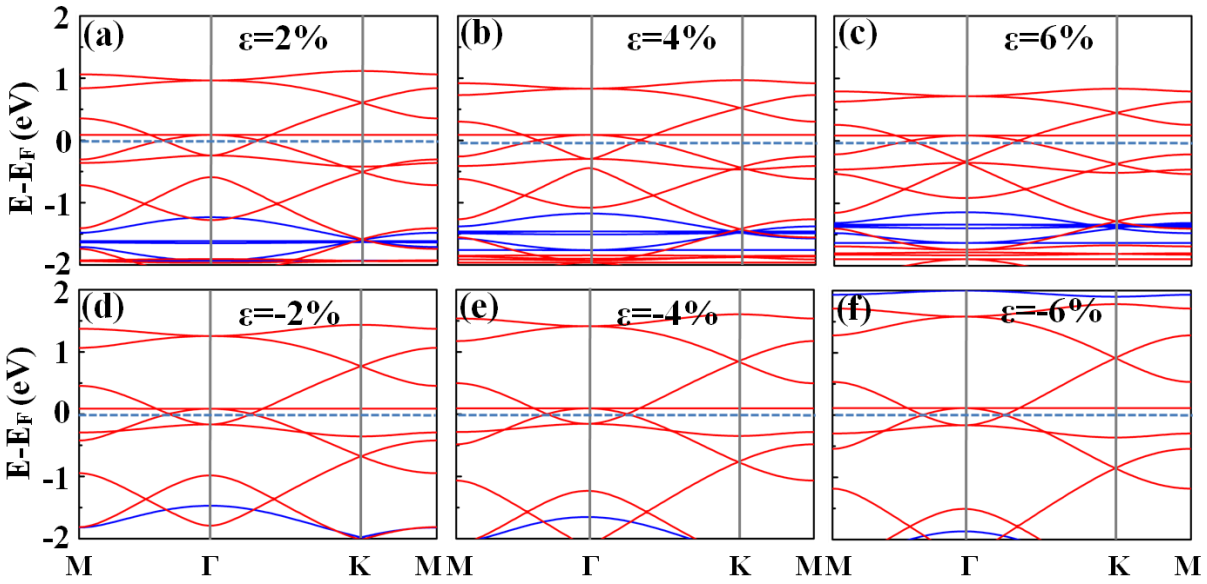

Fig. S5: Band structures of the $Cr_2N_6C_3$ ML under the biaxial tensile (a)-(c) and compressive (d)-(f) strain with different magnitudes, respectively. The SOC interaction is not considered.

Tight-binding Hamiltonian:

For the $d_{x^2-y^2/xy}$-honeycomb and p_z-Kagome combined lattices (Fig. S3), the real and reciprocal lattice vectors are respectively given by

$$\mathbf{a}_1 = a_0(1,0,0),\ \mathbf{a}_2 = a_0\left(-\frac{1}{2},\frac{\sqrt{3}}{2},0\right),\ \mathbf{a}_3 = a_0(0,0,20/a_0);$$

$$\mathbf{b}_1 = \frac{2\pi}{\Omega}(\mathbf{a}_2\times\mathbf{a}_3),\ \mathbf{b}_2 = \frac{2\pi}{\Omega}(\mathbf{a}_3\times\mathbf{a}_1);$$

$$\Omega = |\mathbf{a}_1\cdot(\mathbf{a}_2\times\mathbf{a}_3)|,$$

where a_0 is the optimized lattice constant.

The basis functions can be taken as $|d^{\mathrm{A}}_{x^2-y^2}\rangle$, $|d^{\mathrm{A}}_{xy}\rangle$, $|d^{\mathrm{B}}_{x^2-y^2}\rangle$, $|d^{\mathrm{B}}_{xy}\rangle$, $|p_z^{\mathrm{C1}}\rangle$, $|p_z^{\mathrm{C2}}\rangle$, $|p_z^{\mathrm{C3}}\rangle$. Due to the opposite mirror eigenvalues of the two group orbitals accommodated on the different sublattices, the hopping between the Cr-$d_{x^2-y^2/xy}$ and N-$p_z$orbitals is forbidden and thus the model Hamiltonian can be written as

$$H = H_{\mathrm{h}}(\mathbf{k})\oplus H_{\mathrm{K}}(\mathbf{k})$$

$$= \begin{pmatrix} H_{\mathrm{h}}^{\mathrm{hop}}(\mathbf{k}) + H_{\mathrm{h}}^{\mathrm{SOC}}(\mathbf{k}) & 0 \\ 0 & H_{\mathrm{K}}^{\mathrm{hop}}(\mathbf{k}) + H_{\mathrm{K}}^{\mathrm{SOC}}(\mathbf{k}) \end{pmatrix}. \quad (1)$$

In Eq. (1), the

$$H_{\mathrm{h}}^{\mathrm{hop}}(\mathbf{k}) = \begin{pmatrix} H^{\mathrm{AA}}(\mathbf{k}) & H^{\mathrm{AB}}(\mathbf{k}) \\ H^{\mathrm{BA}}(\mathbf{k}) & H^{\mathrm{BB}}(\mathbf{k}) \end{pmatrix} = \begin{pmatrix} \epsilon_d & 0 & h^{\mathrm{AB}}_{x^2-y^2,x^2-y^2} & h^{\mathrm{AB}}_{x^2-y^2,xy} \\ 0 & \epsilon_d & h^{\mathrm{AB}}_{xy,x^2-y^2} & h^{\mathrm{AB}}_{xy,xy} \\ \dagger & \dagger & \epsilon_d & 0 \\ \dagger & \dagger & 0 & \epsilon_d \end{pmatrix}, \quad (2)$$

where $h^{\mathrm{AB}}_{x^2-y^2,x^2-y^2} = \sum_{\mathrm{i}}[\frac{3}{4}(l_{\mathrm{i}}^2 - m_{\mathrm{i}}^2)^2 V_{dd\sigma} + [l_{\mathrm{i}}^2 + m_{\mathrm{i}}^2 - (l_{\mathrm{i}}^2 - m_{\mathrm{i}}^2)^2]V_{dd\pi} + [n_{\mathrm{i}}^2 + (l^2 - m_{\mathrm{i}}^2)^2/4]V_{dd\delta}]e^{i\mathbf{k}\cdot\boldsymbol{d}_{\mathbf{i}}}$, (3)

$$h^{\mathrm{AB}}_{xy,xy} = \sum_{\mathrm{i}}[3l_{\mathrm{i}}^2 m_{\mathrm{i}}^2 V_{dd\sigma} + (l_{\mathrm{i}}^2 + m_{\mathrm{i}}^2 - 4l_{\mathrm{i}}^2 m_{\mathrm{i}}^2)V_{dd\pi} + (n_{\mathrm{i}}^2 + l_{\mathrm{i}}^2 m_{\mathrm{i}}^2)V_{dd\delta}]\, e^{i\mathbf{k}\cdot\boldsymbol{d}_{\mathbf{i}}}, \quad (4)$$

$$h^{\mathrm{AB}}_{xy,x^2-y^2} = \sum_{\mathrm{i}}[\tfrac{3}{2} l_{\mathrm{i}} m_{\mathrm{i}}(l_{\mathrm{i}}^2 - m_{\mathrm{i}}^2)V_{dd\sigma} + 2l_{\mathrm{i}} m_{\mathrm{i}}(m_{\mathrm{i}}^2 - l_{\mathrm{i}}^2)V_{dd\pi} + [l_{\mathrm{i}} m_{\mathrm{i}}(l_{\mathrm{i}}^2 - m_{\mathrm{i}}^2)/2]V_{dd\delta}]e^{i\mathbf{k}\cdot\boldsymbol{d}_{\mathbf{i}}}.$$

(5)

In Eqs. (2-5), the ϵ_d is the on-site energy of $d_{x^2-y^2/xy}$ orbital, the *l*, *m*, and *n* are the direction cosines, and the $V_{dd\sigma}$, $V_{dd\pi}$, and $V_{dd\delta}$ are the Slater-Koster hopping parameters for the different bonding (σ, π, and δ) between the $d_{x^2-y^2}$ and d_{xy} orbitals. In Eq. (1), the

$$H_{\mathrm{K}}^{\mathrm{hop}}(\mathbf{k}) = -\begin{pmatrix} \epsilon_p & 2t_K\cos[\mathbf{k}\cdot(\boldsymbol{d_1}-\boldsymbol{d_3})/2] & 2t_K\cos[\mathbf{k}\cdot(\boldsymbol{d_2}-\boldsymbol{d_3})/2] \\ 2t_K\cos[\mathbf{k}\cdot(\boldsymbol{d_1}-\boldsymbol{d_3})/2] & \epsilon_p & 2t_K\cos[\mathbf{k}\cdot(\boldsymbol{d_2}-\boldsymbol{d_1})/2] \\ 2t_K\cos[\mathbf{k}\cdot(\boldsymbol{d_2}-\boldsymbol{d_3})/2] & 2t_K\cos[\mathbf{k}\cdot(\boldsymbol{d_2}-\boldsymbol{d_1})/2] & \epsilon_p \end{pmatrix}, \quad (6)$$

where the ϵ_p and t_K are the on-site energy and nearest-neighbor hopping of the p_z orbital, respectively.

The SOC terms in Eq. (1) are given by

$$H_{\mathrm{h}}^{\mathrm{SOC}}(\mathbf{k}) = 2\lambda_1 \begin{pmatrix} 0 & -i & 0 & 0 \\ i & 0 & 0 & 0 \\ 0 & 0 & 0 & -i \\ 0 & 0 & i & 0 \end{pmatrix} \quad (7)$$

and

$$H_{\mathrm{K}}^{\mathrm{SOC}}(\mathbf{k}) = 2i\lambda_2 \begin{pmatrix} 0 & \cos[\mathbf{k}\cdot(\boldsymbol{d_1}-\boldsymbol{d_3})/2] & -\cos[\mathbf{k}\cdot(\boldsymbol{d_2}-\boldsymbol{d_3})/2] \\ -\cos[\mathbf{k}\cdot(\boldsymbol{d_1}-\boldsymbol{d_3})/2] & 0 & \cos[\mathbf{k}\cdot(\boldsymbol{d_2}-\boldsymbol{d_1})/2] \\ \cos[\mathbf{k}\cdot(\boldsymbol{d_2}-\boldsymbol{d_3})/2] & -\cos[\mathbf{k}\cdot(\boldsymbol{d_2}-\boldsymbol{d_1})/2] & 0 \end{pmatrix}. \quad (8)$$